Please use this PDF proof to check the layout of your article. If you would like any changes to be made to the layout, you can leave instructions in the online proofing interface. First, return to the online proofing interface by clicking "Edit" at the top page, then insert a Comment in the relevant location. Making your changes directly in the online proofing interface is the quickest, easiest way to correct and submit your proof.

Please note that changes made to the article in the online proofing interface will be added to the article before publication, but are not reflected in this PDF proof.

Author Query Form

Journal: POLLACK

Article Number: 606.2024.00955

Dear Author,

Please check your proof carefully and mark all corrections at the appropriate place in the proof.

Queries and/or remarks

[Q1]	Please confirm that given names and surnames have been identified correctly and are presented in the desired order and please carefully verify the spelling of all authors' names. Please note that changes in authorship are not allowed in this stage.
[Q2]	Please note that as per style, the ORCID information is recommended for the corresponding author. Hence, please provide ORCID for the corresponding author "Salman Khayoon Aldriasawi". Refer to the site "https://orcid.org/" for more information about ORCID.
[Q3]	Please check the accuracy of the affiliations of each author and make changes as appropriate. Affiliations cannot be changed once the article has been published online.
[Q4]	Please confirm that the provided email "Salman.khayoon@mtu.edu.iq" is the correct address for official communication; else provide an alternate e-mail address to replace the existing one.
[Q5]	Please check acknowledgment/funding information and make sure none is missing and those listed – if any – are accurate. Once the article is published these can only be added/updated in a corrigendum.
[Q6]	For Figure(s) 2 and 3, The image contains text that appears to be important, but is not legible. Please provide a replacement image or detailed guidance on the texts that are to appear in the image.
[Q7]	For Figure(s) 4, The supplied source image has a low resolution (not enough pixels) and the visual quality is not sufficient. Please provide us with an image that has a minimum resolution of 300 dpi in its full size (typically we need a minimum of 900 pixels wide for an image that fits a column width).

AKADÉMIAI KIADÓ

Pollack Periodica • An International Journal for Engineering and Information Sciences

DOI: 10.1556/606.2024.00955

ORIGINAL RESEARCH PAPER

Investigation the effect of surface treatment on the mechanical properties of coating

Salman Khayoon Aldriasawi[1]*, Abbas Nasser Hasein[1], Ashham Muhammed Anead[1] and Barhm Mohamad[2]

[1] Department of Mechanical Engineering, Kut Technical Institute, Middle Technical University, Baghdad, Iraq

[2] Department of Petroleum Technology, Koya Technical Institute, Erbil Polytechnic University, Iraq

Received: October 11, 2023 • Revised manuscript received: January 4, 2024 • Accepted: January 20, 2024

ABSTRACT

The study analyzed surface treatment's impact on mechanical properties of Fe-based amorphous coatings. Specimens underwent six-hour treatments at 670 and 770 °C using vacuum heat. Results revealed distinct mechanical features in the coating: Vickers hardness reached 755, scanning electron microscope images displayed glassy phases, showcasing good wear resistance and compressive residual stresses at around −55 MPa. A remarkable 122% increase in compressive residual stress was noted through combined vacuum heat treatment and sandblasting. Volume wear decreased from the initial 18 to 14 mm^3 after treatment at 670 °C followed by sandblasting, indicating a 30% enhancement in wear resistance. Yet, using vacuum heat treatment at 770 °C negatively impacted the coating's properties.

KEYWORDS

Fe-based amorphous, mechanical properties, sandblast process, vacuum heat treatment

1. INTRODUCTION

Every mechanical or structural component is chosen and created for a specific application. Materials are generally classified into three categories: semi-crystalline, crystalline, and amorphous, based on their structure. Amorphous materials, known for their durability and wear resistance, such as Fe-based amorphous, are extensively used in various fields, including mobile, aeronautical, automotive, and military equipment. To enhance mechanical resilience against stress, different materials and coating techniques, like glass, ceramic, plastic, and elastic materials, are used. Techniques such as thermal spray, sol-gel, electro-deposition, and micro-arc oxidation serve as protective layers against wear, corrosion, and fatigue [1, 2]. High-Velocity Oxygen Fuel (HVOF) is a method that produces high wear resistance and hardness by blasting coating particles at high velocity and low temperature [3].

The kinetic energy of the coating spray significantly impacts the layer properties, increasing fatigue life. For instance, Cr_3C_2 single bond NiCr coating powder, when applied at higher velocities, shows superior fatigue performance compared to uncoated or low-velocity coated steel [4]. FeCrMnCoSi HVOF coating offers effective defence against abrasion, corrosion, and erosion for stainless steel [5]. Optimal fatigue performance is achieved with high-velocity processes and low powder temperature, inducing strong compressive stress near the surface [5–7].

The substrate and coated layer nature affect the residual stresses near the surface, impacting fracture toughness under different loads [8–11]. Coating amorphous materials, like Fe-based amorphous on magnesium alloy, enhances corrosion resistance [12]. Various elements, including Ni, Cr, and rare earth elements, improve tribological properties in coatings [13, 14].

*Corresponding author.
E-mail: Salman.khayoon@mtu.edu.iq

AKJournals

Amorphous materials exhibit special resistance due to their disordered atomic structure, providing wear, corrosion, hardness, sustainability, and high elastic modulus [15–17]. FeBSiNb coating materials resist erosive wear at high temperatures, suitable for power plant use [18]. They lack imperfections like dislocations and grain boundaries [19] and can be produced via multiple techniques, although bulk size is limited [20]. However, due to the absence of slip bands, they are not recommended for structural applications involving tensile or bearing loads [21].

Heat treatment stabilizes amorphous materials and is advised for prepared coating amorphous alloys [22]. Controlled heat treatment of ZrCuAlNiTi metal glass enhances mechanical properties [23]. Heat treatment impacts phase transitions, microstructures, and failure properties in materials like $Co_{69}Fe_4Cr_4Si_{12}B_{11}$ micro-wires before coating [24]. Annealing temperatures influence corrosion and erosion resistance in coated surfaces, increasing friction and wear resistance [25–27]. The heat treatment affects amorphous fraction, which lead to reduce its value with increasing of vacuum temperatures. The hardness, and loses wear rate of heat treated coating layer were increased [28]. Heat treatment is improved the mechanical properties of coating as compared with untreated coating layer [29]. Effects of heat treatment on the mechanical properties of coating were investigated based on the microstructural analysis. The results were indicated increasing by bounding forces and hardness, whereas decreasing of porosity [30].

Shot peening is a widely-used cold working method to improve mechanical properties like fatigue life, hardness, and residual stress [31–33]. It increases the micro-hardness and service life of manufactured components like 5CrNiMo dies [34]. The surface characteristics of the AISI 1045 [35] steel alloy, which are used for wide range of mechanical structures based on its high mechanical performance, optimized by using shot peening process. It is influenced by varying shot peening parameters, the effects figured out by numerical modeling [36–43]. Achieving the best mechanical properties requires a nanostructure at the material's surface [44].

In this study, various surface treatments are used to offer cover layer enhanced mechanical properties than substrate layer of 316L steel alloy. Ball milling is used to characterize amorphous powder. Ball milling is used for 120 h to extract coating material made of amorphous-based Fe, B, C, Cr, Mn, Mo, Si, and W. The stainless steel 316L substrate layer is coated using HVOF method. The coated material is next subjected to a vacuum heat treatment procedure, which is introduced under different values of temperatures at 670–770 °C, in order to obtain the best improvements in the mechanical properties. Further to investigate the impact of sandblasting process on the coating layer, the results of hardness, wear, residual stress, and microstructures are compared with the results of un-sandblasted specimens. The effect of sandblasting process on the bounding force between coating layer and the surface also, is investigated.

2. METHODS AND EXPERIMENTAL

2.1. Preparing coating powder and specimens

Procured from Shandong Runhai Stainless Steel, a 316L plate (40 × 30 × 2 cm) underwent hardness, stress, and microstructure testing using cube-shaped and round specimens as it is shown in Fig. 1. Chemical composition details are in Table 1. The alloy boasts 570 MPa yield stress, 685 MPa ultimate stress, and 300 Vickers Hardness (HV), Fe-based amorphous, from USA-sourced powders (99.9% purity). The various weights of powder components are shown in Table 2, those were created with a 10:1 ratio of components, milled for 120 h at 700 rpm [45, 46]. Specimens, polished and ground, underwent spray drying (150 °C, 0.8% PolyVinyl Alcohol (PVA), 8,000 rpm). Final argon atomization kept powder diameter within +13 to −55 μm. HVOF was chosen for coating due to its advantages, Fig. 2 [4]. Coating layer thickness is measured by electronic micrometer with accuracy value 0.001 mm.

The adhesion force between the substrate and coating layer affects the coating's performance in terms of hardness, strength, and other factors. NiCrAlY bond coat, however, is utilized to enhance adhesive contact [5]. Controlling the substrate's surface roughness is necessary to promote bond coat adhesion [6]. Therefore, the surface of specimens was cleaned, polished, and sandblasted by Silicon Carbide (SiC) paper grit No. 20. The coating process is carried out using a commercial machine (Met-Jet 4l, Metallization, West Midlands, UK) and the HVOF spray technique is utilized under conditions that listed in Table 3, and Fig. 2, which have been understood from prior research [7]. The bounding strength is inversely correlated with the coating layer thickness [8]. The coating layer is 250 μm thick. Standard test method ASTM C633-13:2021 [47] The 250 μm thick coating layer undergoes strength measurement using ASTM C633-13:2021 [47] designed for thermal spray coatings, calculates bounding strength. Two cylindrical specimens, coated and substrate are bonded and tested for stress. Scanning

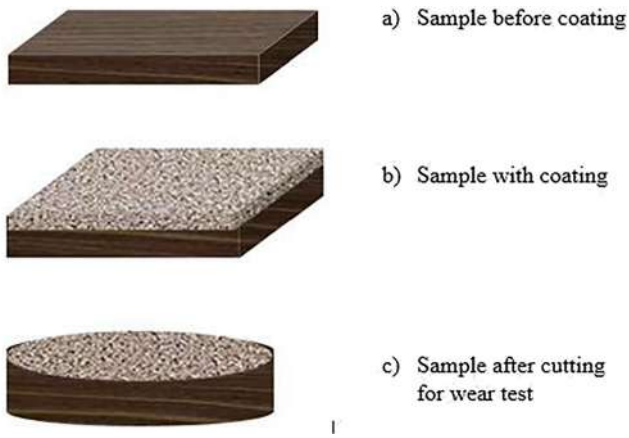

Fig. 1. a) b) Schematic of prepared specimens of substrate with, without coating, and c) schematic of prepared wear specimen after coating (*Source*: Authors' plot)

Table 1. Chemical composition of steel alloy grade 316L (w %) (*Source*: Authors' result)

Fe	Cr	Ni	Mo	Mn	Si	Cu	Co	P	S
Bal.	16.5	12.3	2.3	1.4	0.48	0.4	0.28	0.041	0.002

Table 2. Content of elements which mixing by ball milling machine (*Source*: Authors' result)

Elements	Cr	Fe	Mo	Mn	Si	C	B	W
Weight (g)	183.4	560.3	140.8	1.8	13.9	8.9	32.8	58.7

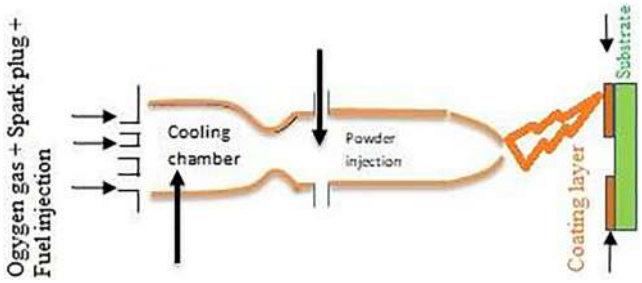

Q6 *Fig. 2.* Schematic of HVOF machine (*Source*: Authors' plot)

Table 3. HVOF parameters during coating process (*Source*: Authors' result)

Parameter	Units	Condition
Oxygen	standard liter per minute (NLPM)	895
Feed rate	gram per min	40
Spraying distance	m	0.39
Carrier gas (argon)	letters per min	8
Combustion pressure	bar	10
Kerosene flow	ml per min.	295
Gun of nozzle	M	0.12

Electronic Microscope (SEM) JSM-6390A, JEOL Ltd, Tokyo, analyzes coating microstructures before and after treatment. Sandblasting studies its impact on coating efficiency, using lab-selected sand (0.6–2.36 mm) to minimize surface roughness.

2.2. Vacuum heat treatment

Coated samples undergo vacuum heat treatment, and treated coatings are compared to untreated ones. Measurements include amorphous powder, coating layers, and steel alloy microstructures. Imperfections during coating application are addressed for a stronger substrate-coating bond through vacuum heat treatment [48–51]. Specimens are heated in a vacuum furnace to the required temperature (670, 770 °C) for 6 h.

2.3. Hardness, wear, and residual stresses, measurement

To comprehend the behavior of prepared powder, coating layer, and substrate during vacuum heat treatment, and sandblasting, mechanical characteristics are assessed [52, 53]; encompassing hardness, wear resistance, and residual stresses. Micro hardness, using HBRVS-187.5 Digital Universal Hardness Tester, is determined pre and post-sandblasting with a Vickers indenter (150 kg load, 10 s). The wear specimen, polished with wet grinding SiC paper (1,600 grit) and ultrasonically cleaned, undergoes wear resistance testing using Tribometer-CETR, UMT-2, USA, with Al_2O_3 ring-disc, loads of 40 and 60 N, and speeds of 0.017, 0.043, and 0.062 m s^{-1} for 45 min at 300 rpm. Residual stresses are gauged via X-Ray Diffraction (XRD) method, XRD 6000, focusing on the surface's depth of 5–15 μm using the sin 2 w method, 3 mm irradiation area, radiation CrKα, and diffraction angle 2θ. Accuracy is ensured by recording residual stress values at five distinct locations.

3. RESULTS

3.1. Structures and thermal stability

Coated of stainless steel plate 316L with dimensions 40 × 30 × 20 is shown in Fig. 3. It was clear that the highest percentage of Fe is present in powder, followed by Cr, Mo, and B elements, in that ratio. It can be seen clearly in Fig. 4a and b of Differential Scanning Calorimeter (DSC), and XRD, the arrangement and coverage of thermal amount of powder before heat treatment is almost have same values of heat, but it is diverging when utilized vacuum heat treatment. For the generated powder, the amount of crystallization temperatures and crystallization enthalpy are listed in Table 4. The convergence among the values of powder, as coting indicated that amorphous structures are same. The particles size of powder is in range of +13 to −55 μm as it is seen by SEM. XRD diffraction of powder, as coating, and at vacuum heat treatment demonstrated that there are no crystalline phase peaks except that of broad amorphous diffraction peak at 44°.

The vacuum heat treatment enhanced the amorphous phase transformation. The considerable amorphous diffraction peak shows that the powders have significant amorphous phase content. In spite of the powder was initially amorphous, as it can be seen in Fig. 5a, the vacuum heat treatment at 670 °C is made the nano-crystallization phases very clear than which under vacuum heat treatment at 770 °C that is formed crystallization phase. The particles, which growth in the argon had semi spherical shapes. The

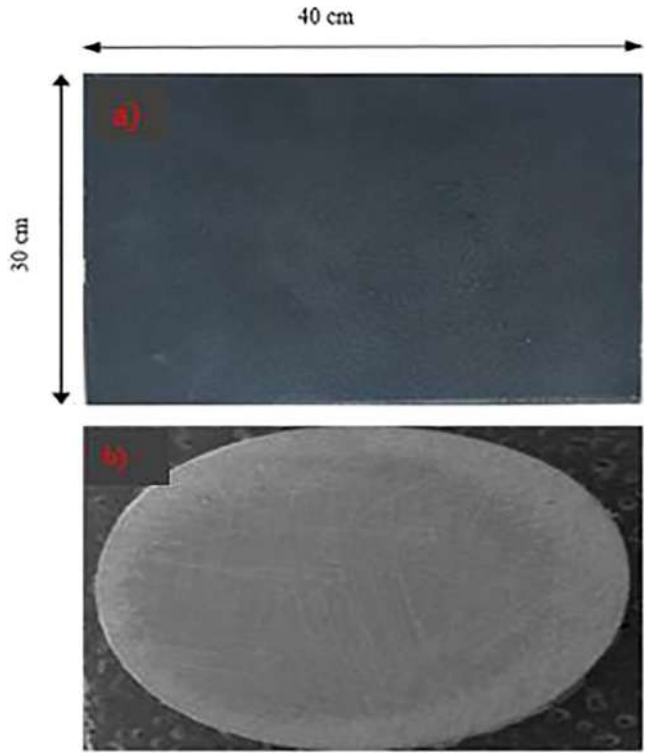

Fig. 3. a) Coated surface of plate, b) sample of wear test with dia. 30 mm (*Source*: Authors' plot)

particles tend to be clumpy with satellites attached. The manner of preparation may be to blame for the clumpy particles. A fine adhesion of substrate and coating layer indicates that the fluidity of the particles is fine. HVOF produces molten powder and a uniform coating layer with very few oxidation and porosity as it can be seen in Fig. 5a–d. Due to high level of homogeneous and stability the vacuum heat treatment 670 °C does not has significant effect on the crystallization of coating. Meanwhile, the crystalline phases formed clearly during vacuum heat treatment at 770 °C which had negative impact on the coating layer. On other hand, after heat treatment at 770 °C, the coating layer tends to weaken, lose adherence and flake. The flattened droplets contained tiny pores, which grew because shrinking of porosity. Due to the phenomenon of losing gas porosity, many pores have formed among flattened droplets. The pores in the surface layer might be result of series sprayed powder in the high speed on the previous amount of coating layer. The defects in the microstructures in Fig. 5d is result of sand blasting process will discuss in next section.

3.2. Sandblast effect on coating

The surface of specimens shot by tiny media (metals, sand, and glass) may have enhanced hardness of surface, compressive RSs, and refined surface structures. During the shot peening process, a force is generated against the direction of shooting. It is generated reactions forces caused compressive residual stresses close to the surface; these forces refine grain size, and increasing surface hardness, and

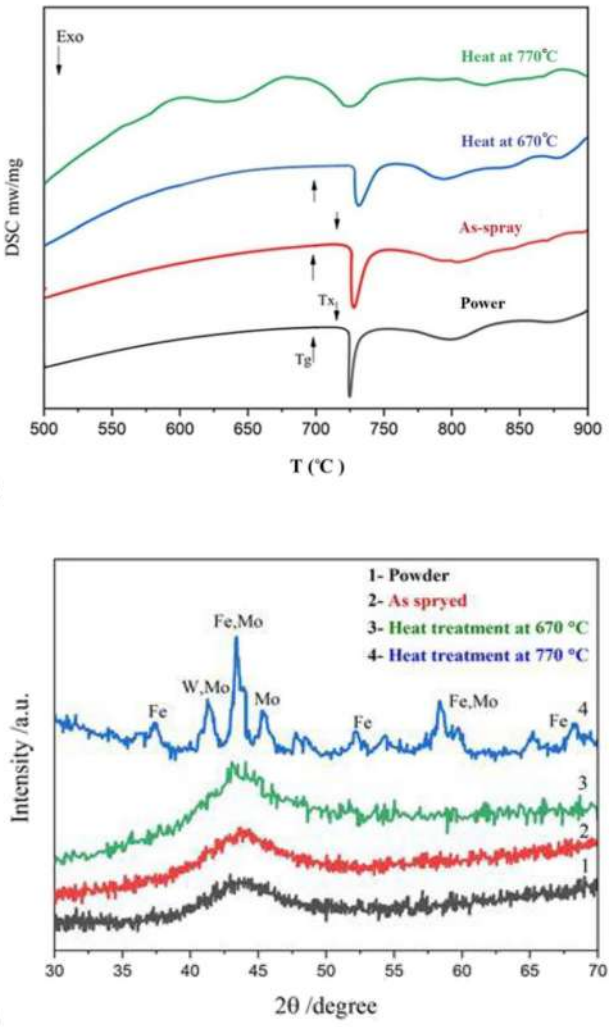

Fig. 4. a) DSC of powder, as sprayed, with vacuum heat treatment 670 °C, and 770 °C, b) XRD of amorphous materials, as - sprayed coating, under vacuum heat treatment 670 °C, and 770 °C (*Source*: Authors' result) Q7

Table 4. Enthalpy of crystallization and temperature of crystallization of coating and powder (*Source*: Authors' result)

Status	Tx [°C]	DH [J g^{-1}]
As produced powder	737.98	−10.23
As coating without treatment	738.34	−11.91
Coating layer with heat treatment 670 °C	738.01	−17.05
Coating layer with heat treatment 770 °C	732.52	−3.828

wear resistance. Heat treatment of coating followed by shot peening process result by high hardness, wear resistance, and low porosity [9, 10]. The peening process has a finite growth limit [11]. The hard shot peening process harm porosity of coating layer. Impacting coating surface result to compact particles of coating layer and splats areas, as well induced compressive residual stresses [12]. Therefore, sandblast instead of shot peening was used in this study.

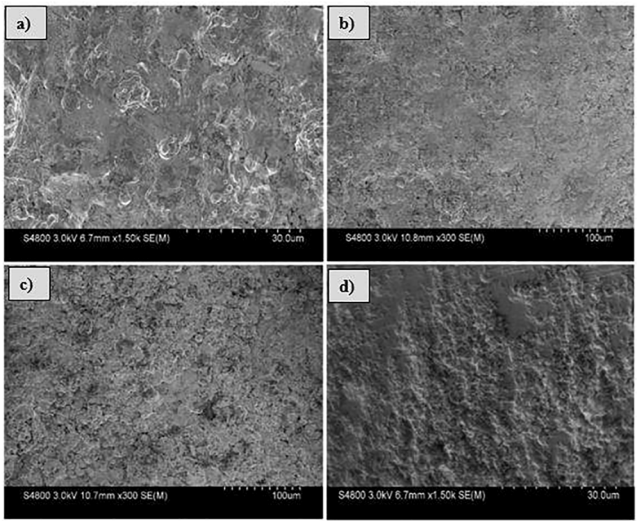

Fig. 5. SEM image of a) as coating layer without treatment, b) coating layer under vacuum heat treatment at 670 °C, c) coating layer with vacuum heat at 770 °C, d) coating with different surface are vacuum treatment, heat treatment and sandblasting process (*Source*: Authors' result)

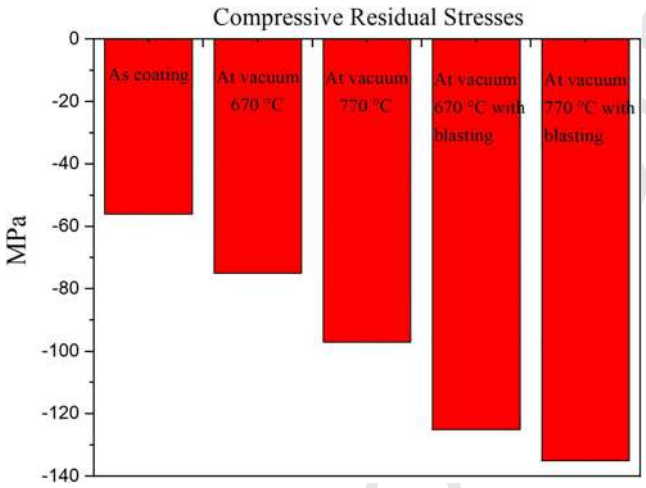

Fig. 6. The relationship of compressive residual stresses with different surface treatment process (*Source*: Authors' result)

As demonstrated in Fig. 5d, the effects of sandblasting process are clear on the surface layer, which remove the crack pitting near surface. In additionally, the bound strength of the coating layer with the substrate and wear resistance was increased. In every instance, sandblasted specimens demonstrated mechanical improvement more favorably than those without a sandblasting treatment. It might belong to the crystallization structure of the coating layer after the surface treatment process, which can controlled during the heat treatment process [2, 10]. Relaxed tension residual stresses were produced as a result of plastic deformation caused by sliding spherical tips on the coated surface [13]. Compressive surface residual stresses were an outcome of the sandblasting process, which further improved hardness and wear resistance Figs 6–11. Figure 7

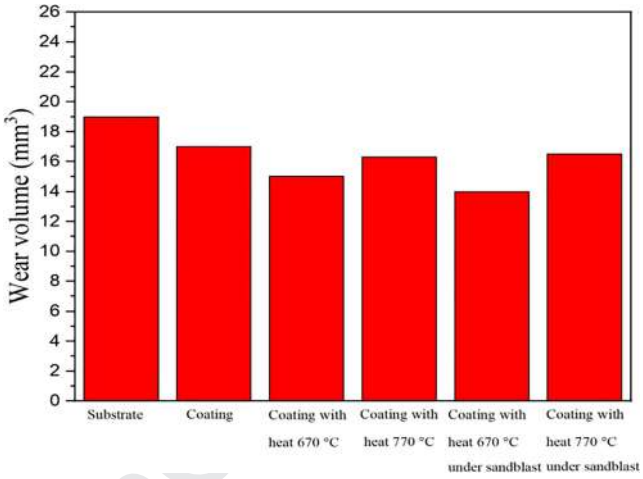

Fig. 7. Effect of surface treatment on the volume wear rate (*Source*: Authors' result)

shows the effect of various surface treatments on the wear rate of steel and coating materials. As it can be seen in Fig. 3b, the sliding contact surface fills with flaws including deep grooves, voids, and cracks. It results from the interaction of adhesive and abrasive of the working surface with sliding load during wear test. The wear rate was increased slightly with increasing spindle speed but had very low sensitivity for the applied load, as it is shown in Fig. 8.

The coating's greatest wear rate resistance was produced at its slowest speed with a 40 N load, approximately 19 mm^3. The wear rate was increased gradually with increasing of spindle speed, as it can be seen in Fig. 8. Vacuum heat treatment and sandblasting significantly reduced the wear rate. The amorphous phase manifested during vacuum heat treatment at 670 °C, and the hardening surface outcome a reduction for wear rate. It is not had significant enhancement after vacuum heat treatment at 670 °C better

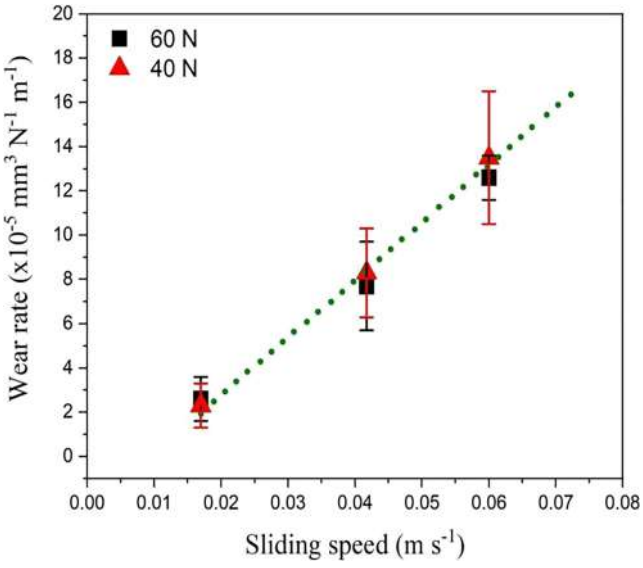

Fig. 8. Relationship of load with the wear rate losses (*Source*: Authors' result)

than at 770 °C, additionally some dark pitting and cracks were elevated which result of formed crystallization at 770 °C, as it is shown in Fig. 9.

The bounding strength is depending on the roughness of surface [12, 14, 15]. The bounding strength is about 27 MPa when surface roughness 5.5 µm, as it can be seen in Fig. 10. During roughness range between 5.5 and 6.4 µm the bounding strength almost same values, but it increased dramatically in the range between 6.4 and 8 µm. At vacuum heat treatment 670 °C the bounding strength was enhanced.

In contrary, the result of vacuum heat treatment at 770 °C was sharp descend. It might be back to formed phases during heat treatment. Amorphous coating of Fe has a high hardness value of around 755 HV. Vacuum heat treatment and sandblasting were used to increase the coating's hardness. Additionally, employing an annealing temperature at 670 °C improved the base coating layer by about 30%, but

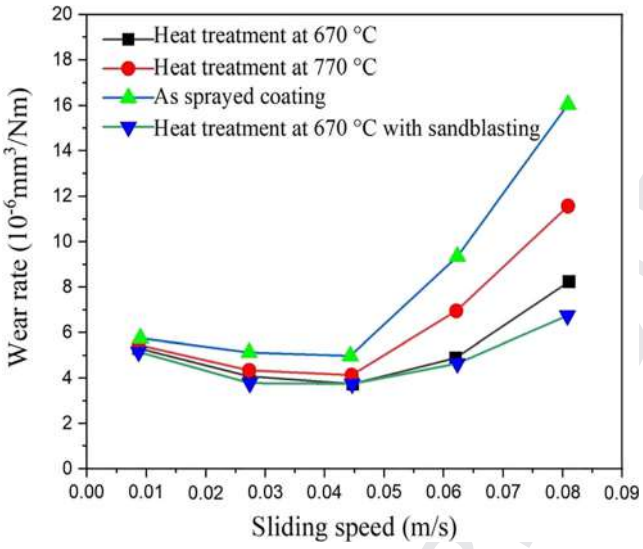

Fig. 9. Relationship between losses of wear rate and sliding speed (*Source*: Authors' result)

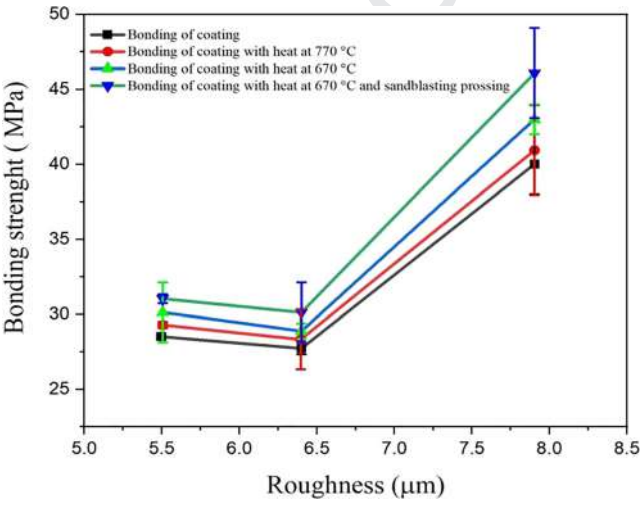

Fig. 10. Effect of surface roughness on the bonding strength under different conditions (*Source*: Authors' result)

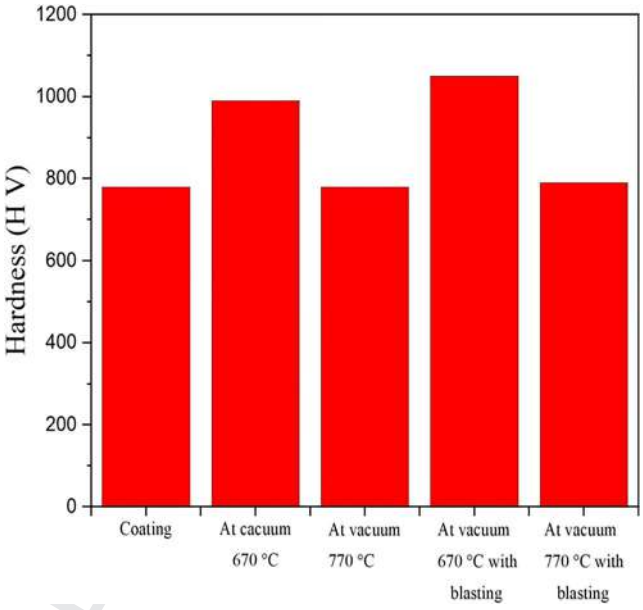

Fig. 11. Effect of surface treatment on the hardness of Fe-based amorphous (*Source*: Authors' result)

utilizing vacuum heat treatment 670 °C followed by sandblasting process improved it by about 37%. Contrarily, as demonstrated in Fig. 11, the improvement of vacuum heat treatment at 770 °C does not exceed 10%, even when followed by a sandblasting process. It can be regarded as a result of the rise of a new phase after vacuum heat treatment at 770 °C.

4. CONCLUSIONS

The article delved into crafting amorphous material and assessing how vacuum heat treatment and sandblasting impact its properties. The conclusions drawn were:

- Using a 120-h ball milling process with high glass content achieves amorphous material characteristics. Coating Fe-based amorphous material through the HVOF method displays potential for diverse applications due to its superior mechanical traits such as hardness, wear resistance, and residual stresses;
- This method yields material with low porosity, robust bonding, and high hardness;
- Vacuum heat treatment 670 °C is improved hardness, wear rate, and microstructures of coating. Vacuum heat treatment at 770 °C the mentioned properties were improved, but mechanical defects were appeared;
- The coating and subsequent sandblasting processes decrease wear, elevate hardness, and induce compressive residual stresses. Hence, precise control of sandblasting parameters is crucial to optimize outcomes in the coating process;
- HVOF technique yields strong bonding. Vacuum heat treatment and sandblasting significantly improve bonding compared to untreated surfaces.

- In the future study, it might be using other coating technique with different parameters and compare the results with current study.
- Using optimization algorithms for coating parameters to obtain optimal mechanical properties.

REFERENCES

[1] T. J. Lin, H. H. Sheu, C. Y. Lee, and H. B. Lee, "The study of mechanical properties and corrosion behavior of the Fe-based amorphous alloy coatings using high velocity oxygen fuel spraying," *J. Alloys Compd.*, vol. 867, 2021, Art no. 159132.

[2] G. Ghosh, A. Sidpara, and P. P. Bandyopadhyay, "Fabrication of mechanically durable slippery surface on HVOF sprayed WC-Co coating," *Surf. Coat. Technol.*, vol. 394, 2020, Art no. 125886.

[3] B. Fotovvati, N. Namdari, and A. Dehghanghadikolaei, "On coating techniques for surface protection: A review," *J. Manufacturing Mater. Process.*, vol. 3, no. 1, 2019, Art no. 28.

[4] W. Fu, Q. Y. Chen, C. Yang, D. L. Yi, H. L. Yao, H. T. Wang, G. C. Ji, and F. Wang, "Microstructure and properties of high velocity oxygen fuel sprayed (WC-Co)-Ni coatings," *Ceramics Int.*, vol. 46, no. 10, Part A, pp. 14940–14948, 2020.

[5] T. Varis, T. Suhonen, O. Calonius, J. Cuban, and M. Pietola, "Optimization of HVOF Cr3C2NiCr coating for increased fatigue performance," *Surf. Coat. Technol.*, vol. 305, pp. 123–131, 2016.

[6] G. Y. Koga, W. Wolf, R. Schulz, S. Savoie, C. Bolfarini, C. S. Kiminami, and W. J. Botta, "Corrosion and wear properties of FeCrMnCoSi HVOF coatings," *Surf. Coat. Technol.*, vol. 357, pp. 993–1003, 2019.

[7] E. S. Puchi-Cabrera, M. H. Staia, M. J. Ortiz-Mancilla, J. G. La barbera-Sos, E. A. O. Perez, C. Villalobos-Gutierrez, S. Bellayer, M. Traisnel, D. Chiot, and J. Lesage, "Fatigue behavior of a SAE 1045 steel coated with Colmonoy 88 alloy deposited by HVOF thermal spray," *Surf. Coat. Technol.*, vol. 205, no. 4, pp. 1119–1126, 2010.

[8] T. Suhonen, T. Varis, S. Dosta, M. Torrell, and J. M. Guilemany, "Residual stress development in cold sprayed Al, Cu and Ti coatings," *Acta Materialia*, vol. 61, no. 17, pp. 6329–6337, 2013.

[9] O. P. Oladijo, L. L. Collieus, B. A. Obadele, and E. T. Akinlabi, "Correlation between residual stresses and the tribological behavior of Inconel 625 coatings," *Surf. Coat. Technol.*, vol. 419, 2021, Art no. 127288.

[10] Š. Houdková and M. Kašparová, "Experimental study of indentation fracture toughness in HVOF sprayed hardmetal coatings," *Eng. Fracture Mech.*, vol. 110, pp. 468–476, 2013.

[11] G. Ghosh, A. Sidpara, and P. P. Bandyopadhyay, "High efficiency chemical assisted nanofinishing of HVOF sprayed WC-Co coating," *Surf. Coat. Technol.*, vol. 334, pp. 204–214, 2018.

[12] S. F. Guo, F. S. Pan, H. J. Zhang, D. F. Zhang, J. F. Wang, J. Miao, C. Su, and C. Zhang, "Fe-based amorphous coating for corrosion protection of magnesium alloy," *Mater. Des.*, vol. 108, pp. 624–631, 2016.

[13] A. List, F. Gärtner, T. Mori, M. Schulze, H. Assadi, S. Kuroda, and T. Klassen, "Cold spraying of amorphous Cu 50 Zr 50 alloys," *J. Therm. Spray Technol.*, vol. 24, pp. 108–118, 2015.

[14] P. Ding, X. J. Liu, J. J. Liu, J. B. Li, H. Q. Li, H. Y. Zhao, J. Y. Duan, and Y. Z. Jiao, "Study on the properties of FeCrNi/CBN composite coating with high velocity arc spraying," *Arabian J. Chem.*, vol. 11, no. 6, pp. 935–941, 2018.

[15] A. Yumashev, B. Ślusarczyk, S. Kondrashev, and A. Mikhaylov, "Global indicators of sustainable development: Evaluation of the influence of the human development index on consumption and quality of energy," *Energies*, vol. 13, no. 11, 2020, Art no. 2768.

[16] D. Nie, E. Panfilova, V. Samusenkov, and A. Mikhaylov, "E-learning financing models in Russia for sustainable development," *Sustainability*, vol. 12, no. 11, 2020, Art no. 4412.

[17] L. Liu and C. Zhang, "Fe-based amorphous coatings: Structures and properties," *Thin Solid Films*, vol. 561, pp. 70–86, 2014.

[18] A. Inoue and A. Takeuchi, "Recent development and application products of bulk glassy alloys," *Acta Materialia*, vol. 59, no. 6, pp. 2243–2267, 2011.

[19] Q. Wang, P. Han, S. Yin, W. J. Niu, L. Zhai, X. Li, X. Mao, and Y. Han, "Current research status on cold sprayed amorphous alloy coatings: A review," *Coatings*, vol. 11, no. 2, 2021, Art no. 206.

[20] J. J. Kruzic, "Bulk metallic glasses as structural materials: A review," *Adv. Eng. Mater.*, vol. 18, no. 8, pp. 1308–1331, 2016.

[21] A. L. Greer, Y. Q. Cheng, and E. Ma, "Shear bands in metallic glasses," *Mater. Sci. Eng. R: Rep.*, vol. 74, no. 4, pp. 71–132, 2013.

[22] V. M. Ievlev, S. V. Kannyikin, T. N. Il'inova, V. V. Vavilova, S. B. Kushchev, D. V. Serikov, and A. S. Baikin, "Heat treatment-and lamp processing-induced structural transformations of an amorphous Fe 77 B 7 Nb 2.1 Si 13 Cu 0.9 alloy and non-monotonic behavior of its mechanical properties," *Inorg. Mater.*, vol. 55, pp. 659–668, 2019.

[23] N. Kang, P. Coddet, H. Liao, and C. Coddet, "The effect of heat treatment on microstructure and tensile properties of cold spray Zr base metal glass/Cu composite," *Surf. Coat. Technol.*, vol. 280, pp. 64–71, 2015.

[24] I. V. Kozlov, G. N. Elmanov, K. E. Prikhodko, L. V. Kutuzov, B. A. Tarasov, V. V. Mikhalchik, R. D. Svetogorov, V. S. Mashera, E. S. Gorelikov, and S. A. Gudoshnikov, "The evolution of structure and magnetoimpedance characteristics of amorphous $Co_{69}Fe_4Cr_4Si_{12}B_{11}$ microwires under heat treatment," *J. Magnetism Magn. Mater.*, vol. 493, 2020, Art no. 165681.

[25] Z. B. Zheng, Y. G. Zheng, W. H. Sun, and J. Q. Wang, "Effect of heat treatment on the structure, cavitation erosion and erosion–corrosion behavior of Fe-based amorphous coatings," *Tribology Int.*, vol. 90, pp. 393–403, 2015.

[26] S. B. Pitchuka, B. Boest, C. Zhang, D. Lahiri, A. Nieto, G. Sundararajan, and A. Agarwall, "Dry sliding wear behavior of cold sprayed aluminum amorphous/nanocrystalline alloy coatings," *Surf. Coat. Technol.*, vol. 238, pp. 118–125, 2014.

[27] H. Al-Abboodi, H. Fan, I. A. Mhmood, and M. Al-Bahrani, "The dry sliding wear rate of a Fe-based amorphous coating prepared on mild steel by HVOF thermal spraying," *J. Mater. Res. Technol.*, vol. 18, pp. 1682–1691, 2022.

[28] F. Huang, J. J. Kang, W. Yue, X. B. Liu, Z. Q. Fu, L. N. Zhu, D. S. She, G. Z. Ma, H. D. Wang, J. Liang, W. Weng, and C. B. Wang, "Effect of heat treatment on erosion–corrosion of Fe-based amorphous alloy coating under slurry impingement," *J. Alloys Compd.*, vol. 820, 2020, Art no. 153132.

[29] Z. B. Zheng, Y. G. Zheng, W. H. Sun, and J. Q. Wang, "Effect of heat treatment on the structure, cavitation erosion and erosion–corrosion behavior of Fe-based amorphous coatings," *Tribology Int.*, vol. 90, pp. 393–403, 2015.

[30] R. K. Sharma, R. K. Das, and S. R. Kumar, "Microstructure, mechanical and erosion wear analysis of post heat treated iron alloy based coating with varying chromium," *Mater. Sci. Eng. Technol.*, vol. 52, no. 11, pp. 1173–1184, 2021.

[31] E. Maleki and O. Unal, "Optimization of shot peening effective parameters on surface hardness improvement," *Met. Mater. Int.*, vol. 27, pp. 3173–3185, 2021.

[32] E. Maleki, G. H. Farrahi, K. R. Kashyzadeh, O. Unal, M. Gugaliano, and S. Bagherifard, "Effects of conventional and severe shot peening on residual stress and fatigue strength of steel AISI 1060 and residual stress relaxation due to fatigue loading: Experimental and numerical simulation," *Met. Mater. Int.*, vol. 27, pp. 2575–2591, 2021.

[33] E. Maleki, G. H. Farrahi, and K. Sherafatnia, "Application of artificial neural network to predict the effects of severe shot peening on properties of low carbon steel," in *Machining, Joining and Modifications of Advanced Materials*, vol. 61, Springer, 2016, pp. 45–60.

[34] S. Bagherifard, R. Ghelichi, and M. Guagliano, "A numerical model of severe shot peening (SSP) to predict the generation of a nanostructured surface layer of material," *Surf. Coat. Technol.*, vol. 204, no. 24, pp. 4081–4090, 2010.

[35] Z. Jia and J. J. Ji, "Influence analysis of shot peening on hot forging die," *Int. J. Adv. Manufacturing Technol.*, vol. 90, pp. 1779–1787, 2017.

[36] E. Maleki and O. Unal, "Roles of surface coverage increase and re-peening on properties of AISI 1045 carbon steel in conventional and severe shot peening processes," *Surf. Inter.*, vol. 11, pp. 82–90, 2018.

[37] S. M. H. Gangaraj, M. Guagliano, and G. H. Farrahi, "An approach to relate shot peening finite element simulation to the actual coverage," *Surf. Coat. Technol.*, vol. 243, pp. 39–45, 2014.

[38] B. Li, Z. Qin, H. Xue, Z. Sun, and T. Gao, "Optimization of shot peening parameters for AA7B50-T7751 using response surface methodology," *Simulation Model. Pract. Theor.*, vol. 115, 2022, Art no. 102426.

[39] M. Hassanzadeh and S. E. M. Torshizi, "Multi-objective optimization of shot-peening parameters using design of experiments and finite element simulation: A statistical model," *J. Appl. Comput. Mech.*, vol. 8, no. 3, pp. 838–852, 2022.

[40] X. Wang, Z. Wang, G. Wu, J. Gan, Y. Yang, H. Huang, J. He, and H. Zhong, "Combining the finite element method and response surface methodology for optimization of shot peening parameters," *Int. J. Fatigue*, vol. 129, 2019, Art no. 105231.

[41] G. I. Mylonas and G. Labeas, "Numerical modeling of shot peening process and corresponding products: residual stress, surface roughness and cold work prediction," *Surf. Coat. Technol.*, vol. 205, no. 19, pp. 4480–4494, 2011.

[42] Y. S. Nam, Y. I. Jeong, B. C. Shin, and J. H. Byun, "Enhancing surface layer properties of an aircraft aluminum alloy by shot peening using response surface methodology," *Mater. Des.*, vol. 83, pp. 566–576, 2015.

[43] S. M. Hassani-Gangaraj, K. S. Cho, H. J. L. Voigt, M. Guagliano, and C. A. Schuh, "Experimental assessment and simulation of surface nanocrystallization by severe shot peening," *Acta Materialia*, vol. 97, pp. 105–115, 2015.

[44] V. H. Nguyen, O. T. H. Nguyen, D. V. Dudina, V. V. Le, and J. S. Kim, "Crystallization kinetics of Al-Fe and Al-Fe-Y amorphous alloys produced by mechanical milling," *J. Nanomater.*, vol. 2016, Art no. 1909108.

[45] L. Pawlowski, *The Science and Engineering of Thermal Spray Coatings*. John Wiley & Sons, 2008.

[46] M. M. Khorramirad, M. R. Rahimipour, S. M. M. Hadavi, and K. Shirvani, "Preoxidation of bond coat in IN-738LC/NiCrAlY/LaMgAl11O19 thermal barrier coating system," *Ceramics Int.*, vol. 44, no. 18, pp. 22080–22091, 2018.

[47] *ASTM C633-13:2021*, Standard Test Method for Adhesion or Cohesion Strength of Thermal Spray Coatings, ASTM International, 2021.

[48] S. Vignesh, K. Shanmugam, V. Balasubramanian, and K. Sridhar, "Identifying the optimal HVOF spray parameters to attain minimum porosity and maximum hardness in iron based amorphous metallic coatings," *Defence Technol.*, vol. 13, no. 2, pp. 101–110, 2017.

[49] E. Hejrani, D. Sebold, W. J. Nowak, G. Mauer, D. Naumenko, R. Vassen, and W. J. Quadakkers, "Isothermal and cyclic oxidation behavior of free standing MCrAlY coatings manufactured by high-velocity atmospheric plasma spraying," *Surf. Coat. Technol.*, vol. 313, pp. 191–201, 2017.

[50] Y. F. Tao, J. Li, J. H. Lv, and L. F. Hu, "Effect of heat treatment on residual stress and wear behaviors of the TiNi/Ti2Ni based laser cladding composite coatings," *Opt. Laser Technol.*, vol. 97, pp. 379–389, 2017.

[51] Z. Zhou, J. Shang, Y. Chen, X. Liang, B. Shen, and Z. Zhang, "Synchronous shot peening applied on HVOF for improvement on wear resistance of Fe-based amorphous coating," *Coatings*, vol. 10, no. 2, 2020, Art no. 187.

[52] F. M. Kadhim, M. S. Al-Din Tahir, and A. T. Naiyf, "The effect of vibrations on the mechanical properties of laminations," *Pollack Period.*, vol. 17, no. 1, pp. 62–65, 2022.

[53] M. Petrik and K. Jármai, "Comparison of optimized steel frame structures," *Pollack Period.*, vol. 17, no. 2, pp. 109–114, 2022.